Macromolecules

pubs.acs.org/Macromolecules Article

Rheological Properties of Concentrated Sodium Polystyrenesulfonate in Aqueous Salt Solutions

Anish Gulati, Aijie Han, Ralph H. Colby, and Carlos G. Lopez*

Cite This: https://doi.org/10.1021/acs.macromol.4c00542 Read Online

ACCESS | Metrics & More | Article Recommendations | Supporting Information

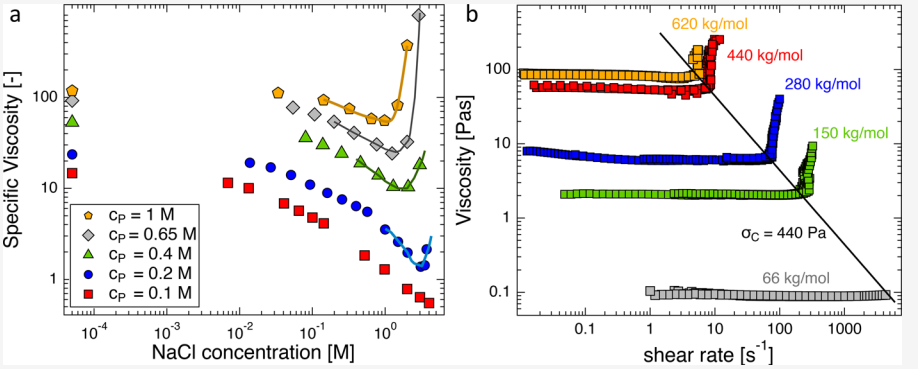

ABSTRACT: We study the conformational and flow properties of sodium polystyrenesulfonate in aqueous NaCl solutions in the high polymer, high added-salt region using rheology and small angle neutron scattering (SANS). For low salt concentrations, the specific viscosity decreases with added salt as expected. At very high salt, however, the specific viscosity is found to rapidly increase with increasing added-salt concentration (c_s). This indicates that addition of salt modifies the system in ways other than simply decreasing the electrostatic screening length. Beyond a critical shear stress of around 400 Pa, independent of molar mass, solutions display strong shear thickening reminiscent of shear-induced gelation. Scaling laws for the zero shear rate viscosity and critical shear rate with molar mass, polymer and added-salt concentration are established and compared to similar behavior observed for other systems. SANS experiments using the zero-average-contrast technique reveal that the chain size monotonically decreases with increasing added salt concentration, indicating that the increases in specific viscosity cannot be assigned to chain expansion. Our results indicate that NaPSS, usually thought to be a model polyelectrolyte system, displays complex and unexpected rheological behavior when both the polymer and added salt concentration approach the molar range, where the Debye screening length becomes smaller than the Bjerrum length.

INTRODUCTION

Polyelectrolytes are polymers with ionic groups along their backbones. They share properties both with simple electrolytes and with nonionic polymers. In salt-free polar solvents, counterions dissociate from the polymer, leading to strong repulsion between like-charged groups along the backbone via long-ranged electrostatic forces, and chains adopt highly extended configurations.[1,2] Their thermodynamic properties are controlled by dissociated counterions, leading to osmotic pressures several orders of magnitude larger than neutral polymers[3−5] and phase boundaries which are largely independent of the chain molar mass, a unique feature among polymeric systems.[6] The rheology of salt-free polyelectrolytes displays several unusual features, including the existence of a broad concentration range over which chains interpenetrate but do not entangle.[1,5,7−17] By contrast, in nonpolar media with low permittivity, the so-called ionomer regime, dipolar attraction between groups with condensed counterions dominates.[18−21] Temporary associations between chains increase the relaxation times in solutions and in the bulk state, yielding markedly different properties from those of polyelectrolytes.[22] Understanding the crossover between these two regimes remains challenging because it involves the balance of dipolar attraction, electrostatic repulsion and the solvation forces for the polymer backbone, ionic groups and counterions.[18−21,23]

When a salt is added to the solvent media, the mobile ions preferentially locate themselves around oppositely charged ones, leading to Debye−Hückel type screening, with a characteristic spatial range approaching the Debye screening

Received: March 8, 2024
Revised: April 29, 2024
Accepted: May 29, 2024

length κ^{-1}. For sufficiently high ionic strengths, electrostatics are predicted to become short-ranged and their effects are similar to excluded volume interactions in nonionic polymers.[1,24,25] The analogy between polyelectrolytes in excess salt and neutral polymers in good solvent is supported by extensive data sets for the conformational and hydrodynamic properties of dilute polyelectrolytes.[2,26−33] Data for nondilute solutions, which generally cover only modestly high polymer and added salt concentrations, broadly support this view.[8,34−36]

The behavior of polyelectrolytes at high polymer and high added salt concentrations (≃ molar) remains largely unexplored. In this article, we report rheological measurements for aqueous solutions of sodium polystyrenesulfonate (NaPSS) with added sodium chloride (NaCl), the canonical model polyelectrolyte system. While dilute and modestly concentrated NaPSS solutions in excess NaCl conform to the widely accepted view of neutral polymer-like behavior,[2,26−33] we observe several unexpected phenomena in the high added salt, high polymer concentration region: 1) the specific viscosity of solutions *increases* with increasing added salt concentration. 2) The specific viscosity scales with molar mass following the reptation exponent of $\eta_{sp} \propto M_w^3$ in excess salt, and $\eta_{sp} \propto M$ (Rouse) in DI water, 3) Solutions display strong and sudden shear *thickening* behavior reminiscent of shear-induced gelation and discontinuous shear thickening of colloids[37,38] that is typically attributed to jamming, 4) Step strain-rate experiments show that beyond a critical shear rate, the apparent viscosity of solutions becomes unstable after an induction time, the value of which depends on the applied shear rate.

These results demonstrate that while the polyelectrolyte in excess salt-neutral polymer analogy holds well in the dilute polymer concentration region and the semidilute regime with not too much added salt, the role of added salt in concentrated polyelectrolyte solutions goes beyond the screening effect and causes the emergence of unusual rheological phenomena. Thus, even simple systems such as NaPSS/NaCl/H_2O solutions display complex flow properties. While the molecular origin underpinning the sharp increases in the apparent viscosity at high concentrations remains unclear, our results indicate the presence of attractive forces in the concentrated polymer and added salt regime. The NaPSS system combines two features that are commonly found across systems displaying such type of rheological behavior, namely the presence of both electrostatic and hydrophobic interactions.[39,40]

MATERIALS AND METHODS

Data. All rheological and neutron scattering data are provided in a spreadsheet appended to the Supporting Information.

Chemicals. NaPSS for the different molar masses was purchased from Polymer Standards Service (Mainz, Germany). The polymers were prepared by sulfonation of polystyrene and purified by ultrafiltration. The details of their characterization can be found in refs.[16,36,41] A deuterated polystyrenesulfonate with N = 750 was also supplied by Polymer Standards Service. NaCl with purity ∼99.9% (Grade: ACS, Reagent. Ph. Eur) and the viscosity standard oil, S3 (Product no. 99472), used to create the seal around the sample on the rotational rheometer were obtained from VWR. NaCl with purity ∼99.5% (Grade: BioReagent) from Sigma-Aldrich was used for the sample for the measurement in Figure 3. Dialysis tubings manufactured by Spectra/Por with MWCO 3.5 kDa, 6−8 kDa and 12−15 kDa were purchased from VWR. D_2O (99.9% isotopic purity) was purchased from Deutero.

Polymer Purification. The NaPSS was purified by dialyzing it against DI water. The dialysis baths were regularly exchanged until an equilibrium bath conductivity of below 2 μS cm^{-1} was attained. The maximum conductivity was determined by measuring the equilibrium conductivity of DI water when exposed to the atmosphere. The DI water used had an initial conductivity of 0.06 μS cm^{-1}, which went up to the threshold value, presumably due to the formation of carbonic acid due to the absorption of CO_2 from the atmosphere.[17,34] These dialyses were carried out as a precautionary measure to remove any residual ionic impurities from the polymer. In practice, the conductivity never went beyond the threshold, in which case the dialyses were carried out for 24 h. The dialyzed solutions were then freeze-dried under a vacuum pressure of ∼0.4 mbar for 3 to 4 days.

Small Angle Neutron Scattering. SANS measurements were carried out at the SANS2D beamline at the ISIS neutron facility (Chilton, UK). The sample-to-detector distance was set at 4 m. A white neutron beam with an average wavelength of 6 Å was used. Samples were measured in 2 mm quartz cells and reduced using standard protocols. All measurements were carried out using 71/29 D_2O/H_2O by mole fraction as a solvent and equal number concentrations of h-PSS and d-PSS. This corresponds to the zero-average contrast condition.[42]

Sample Preparation. Samples for viscosimetry or rheology were prepared in 2 mL polypropylene vials. Prior to use, these were carefully washed using DI water and dried in an oven at 60 °C. The weighing balance used had a typical error of ±0.05 mg. The densities of water, NaCl and NaPSS were taken to be 1, 2.16, and 1.65 g cm^{-3}. The density of NaPSS has been retrieved from literature[43] where it has been determined from its partial molar volume.

Measurement Methods. The procedures for sample preparation and loading into the rheometer were found to influence the rheological properties of NaPSS/NaCl/H_2O solutions. Four methods were evaluated until a final protocol was established referred to as 'Method 2' in the Supporting Information. All the data presented in the main text are for samples prepared by method 2. Data for samples prepared using the other methods are discussed in the SI.

Rheology. All the rheological measurements reported in the main paper were carried out using a Kinexus stress-controlled rotational rheometer from Netzsch. A 40 mm cone−plate geometry (θ = 1°, sample volume = 0.3 mL) with a solvent trap was used. The instrument was routinely calibrated by running a 20 min torque mapping in air. The sample temperature of 25 °C was maintained on this rheometer using a Peltier bottom plate with enclosed top. A strain-controlled rheometer, RFS3 from TA Instruments, was used for the measurements shown in Figure S6 in the Supporting Information.

Birefringence Measurements. Birefringence measurements under shear flow were performed on a stress-controlled MCR502 rheometer (Anton Paar), equipped with shear-induced polarized light imaging (SIPLI). The geometry consisted of a bottom glass plate and a metal top plate with a diameter of 25 mm. More details on the instrument setup can be found in ref [44]. The gap was set to 25 and 50 μm. The sample was prepared following method 1 and the measurement was carried out in the presence of an oil trap but no N_2 flow. The measurements on a c = 0.8 M and c_s = 2.3 M sample were carried out in the Newtonian region and in the shear thickening region (up to viscosities ≃ × 4 than the Newtonian value). These did not result in any measurable birefringence signal.

Viscosimetry. A Lovis 2000 M rolling-ball viscometer from Anton Paar was used for some measurements, which were found to agree with the rheometer data. This confirms that the air−water or oil−water interfaces, which are present in the rheometer but not in the Lovis, do not significantly influence our results. Two different capillaries with internal diameters of 1.59 mm and 1.8 mm were used for low and high-viscosity samples, respectively. The dynamic viscosities were determined from the time taken by a steel ball to roll a fixed distance across the capillary at an angle of 30°. The closed setup prevented any evaporation and eliminated any role of the air−water interface, which is always present in a rotational rheometer for a cone−plate geometry. The instrument was calibrated using a viscosity standard procured from VWR.

https://doi.org/10.1021/acs.macromol.4c00542
Macromolecules XXXX, XXX, XXX−XXX

pH Measurements. The pH measurements were carried out at room temperature using the Metrohm 744 pH meter. The instrument was calibrated before the measurements using two standards with pH = 4 and 10, respectively, and verified using a standard with pH = 7. Tests with litmus paper were used for selected samples to check the accuracy of the pH meter readings.

RESULTS

Sample Stability and Solubility. The stability of the NaPSS samples was investigated. It was found that NaPSS degraded in aqueous solutions in the presence of NaCl over long time scales, indicated by the solutions turning amber. This amber coloration was observed after a few months in a 1 molar aqueous NaPSS (150 kg/mol) sample with c_s = 2.6 M. The solution had turned acidic and the pH of this degraded sample was found to be 1.68. Similar degradation for HPSS has also been reported by Reddy and Marinsky.[45] The data reported here are for solutions which were stable over shorter time scales and the measurements were carried out as soon as the samples dissolved so they did not have a chance to degrade, as determined visually and by measuring the viscosity as a function of time.

In 2.5 M NaCl, NaPSS was found to be soluble at low and high polymer concentrations. At intermediate concentrations ($c \simeq 0.2-0.5$ M), NaPSS did not fully dissolve (see SI for further details). This behavior is consistent with the closed-loop phase diagram for polyvinyl sulfate reported by Eisenberg and co-workers.[46−48] An important aspect of this study is that the solutions with unexpected results are never far from a phase boundary.

Rheology. Stable measurements in the cone and plate geometry were usually obtained within 20 s of imposing a particular shear stress. It took about 3 s for the instrument to reach the target shear rate, followed by 6 to 7 s for stress equilibration. The instrument was programmed to record 10 s of viscosity data with a variation of less than 1% and average over that period to obtain the final viscosity for a given shear rate. The measurement program had a cutoff time of 60 s for most of the measurements (180 s for the others). However, the acquisition times for each point in the reported data were within these limits (<45 s). This confirms that the viscosity data reported in the following (except for Figure 3 as discussed below) correspond to steady-state.

Figure 1a plots the specific viscosity of a NaPSS sample with M_w = 271 kg/mol as a function of c_s for different polymer concentrations c. The specific viscosity is calculated from the zero-shear viscosity, which in turn is determined by averaging the apparent solution viscosity over a range of shear rates in the low-shear Newtonian regime. A residual salt concentration of $\sim 7.4 \times 10^{-5}$ M is considered under no added-salt condition as estimated in a previous work.[36] The specific viscosity initially decreases with added salt content, in line with the predictions of the scaling theory.[1,36] The data for c_s < 1 M and c < 1 M were fitted to the scaling model of Dobrynin et al.,[49] see ref [36] for details. In brief, it was found that the scaling model could capture the experimentally observed trends for the viscosity as a function of polymer and added salt concentrations, but the obtained structural parameters do not always match estimates for these quantities from scattering data. Beyond a critical salt concentration ($c_{s,u}$), the trend in Figure 1 reverses, as η_{sp} increases with increasing c_s. The value of $c_{s,u}$ is found to be independent of the degree of

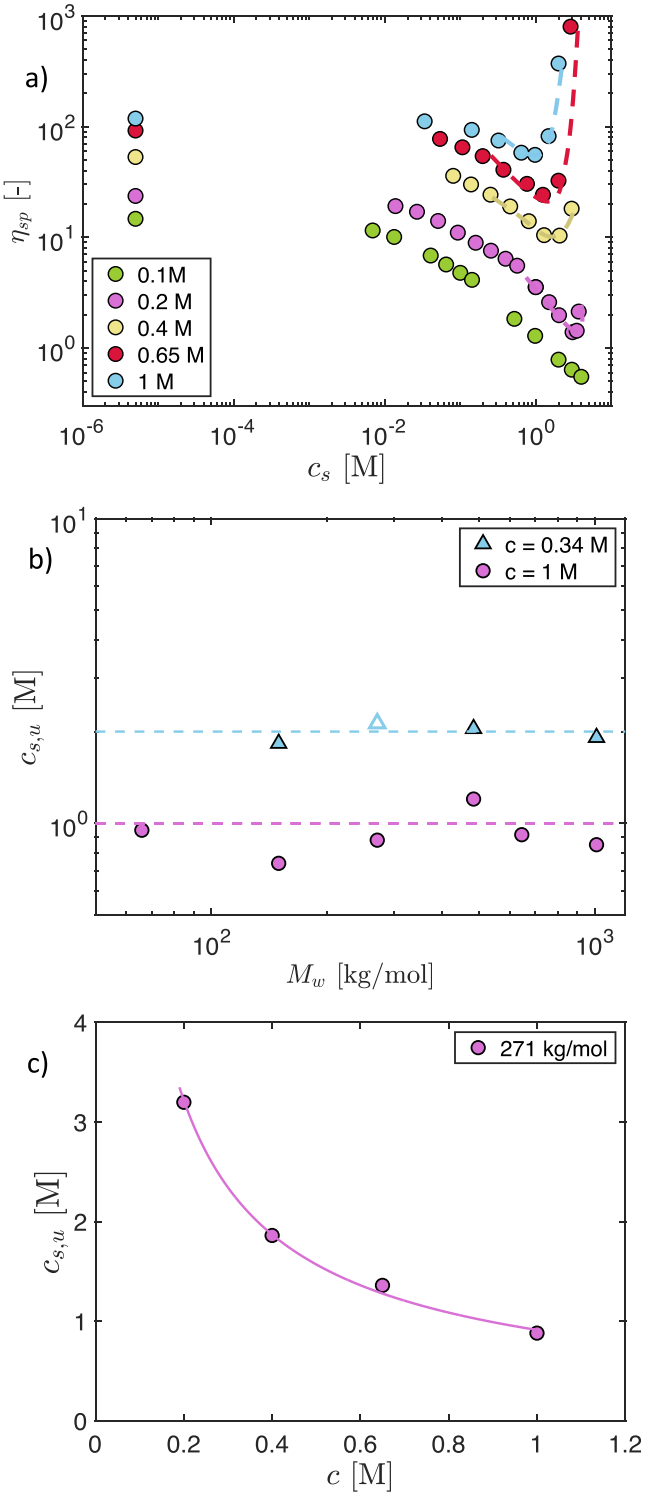

Figure 1. a) Specific viscosity as a function of added NaCl concentration for NaPSS with an M_w = 271 kg/mol at different polymer concentrations, indicated on the legend. The dashed lines are guides to the eye. Some of these measurements were reported in a previous publication.[36] b) Upturn salt concentration ($c_{s,u}$) as a function of M_w at c = 0.34 M and c = 1 M. The dashed lines represent $c_{s,u}$ = 1 M (pink) and $c_{s,u}$ = 2 M (blue). The hollow symbol is an interpolated value for M_w = 271 kg/mol at c = 0.34 M using the trend-line in part c. c) Upturn salt concentration ($c_{s,u}$) as a function of the polymer concentration for NaPSS with M_w = 271 kg/mol. The solid line is a best-fit power-law giving $c_{s,u} \sim c^{-0.78}$.

https://doi.org/10.1021/acs.macromol.4c00542
Macromolecules XXXX, XXX, XXX−XXX

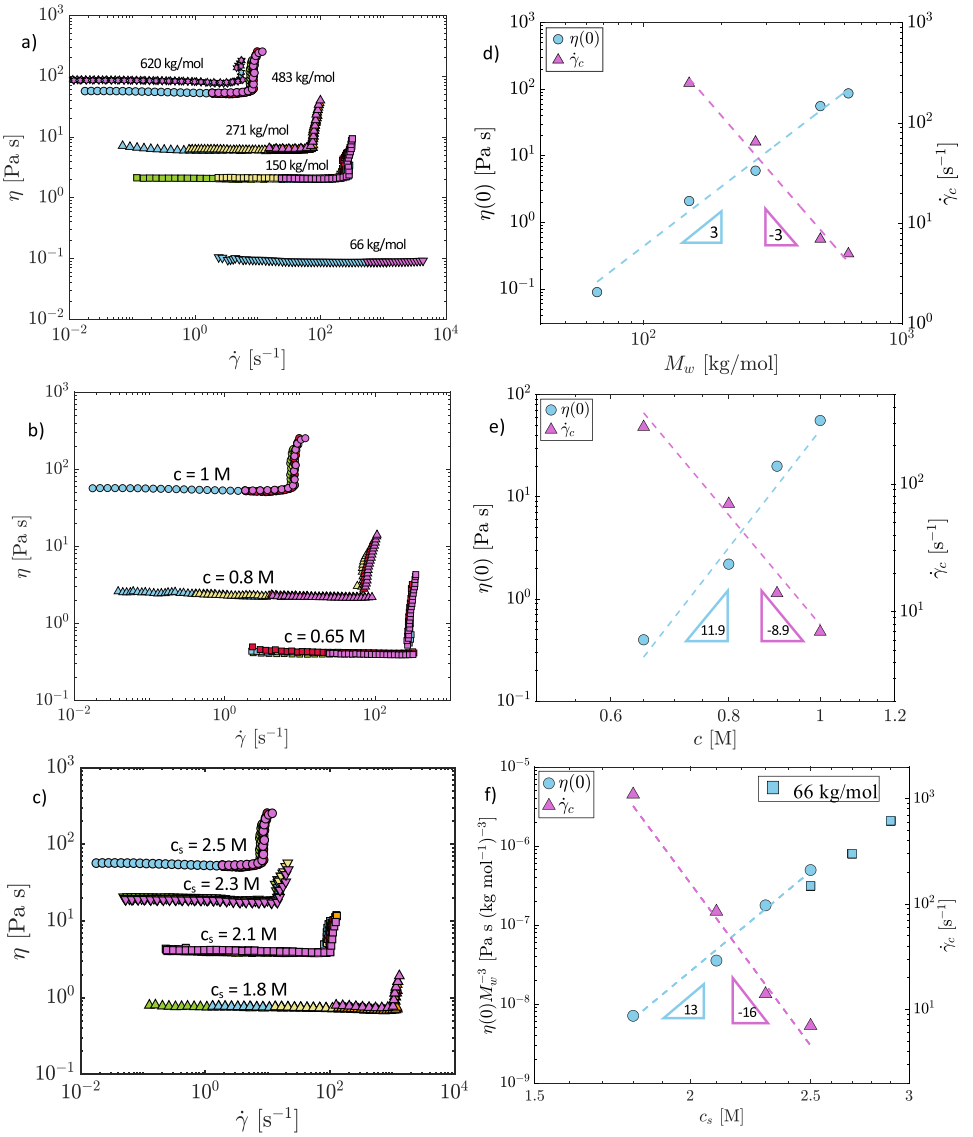

Figure 2. a) Viscosity (η) vs shear rate ($\dot{\gamma}$) flow curves for NaPSS with different M_w at c = 1 M and c_s = 2.5 M. η vs $\dot{\gamma}$ flow curves for NaPSS with M_w = 483 kg/mol at b) c_s = 2.5 M for different c and c) c = 1 M for different c_s. The different colors correspond to different measurements for the same sample loaded once. Zero-shear viscosity ($\eta(0)$) and critical shear rate ($\dot{\gamma}_c$) as functions of d) M_w at c = 1 M and c_s = 2.5 M, e) c at c_s = 2.5 M for M_w = 483 kg/mol. f) $\eta(0)$ (normalized by $(M_w)^3$) (circles) and $\dot{\gamma}_c$ (triangles) as functions of c_s at c = 1 M for M_w = 483 kg/mol and M_w = 66 kg/mol (squares). The numbers in the triangles are the best-fit exponents only for the data for NaPSS with M_w = 483 kg/mol.

polymerization, as shown in Figure 1b and a decreasing function of the polymer concentration with

$$c_{s,u} \simeq 0.91c^{-0.78} \quad (1)$$

see Figure 1c. No upturn is observed for c = 0.1 M for c_s as high as 4 M, beyond which NaPSS begins to precipitate. This observation is our first hint that the interesting data at high c_S in Figure 2 might be the consequence of being close to a phase transition.

Representative flow curves for samples with $c_s \gtrsim c_{s,u}$, plotted in Figure 2a-c, reveal unusual rheological properties. At low shear rates, Newtonian or weak shear thinning is observed, which is the standard behavior of semidilute neutral polymer or polyelectrolyte solutions.[5,7,34,50−53] Beyond a critical shear rate ($\dot{\gamma}_c$), the apparent viscosity displays a strong upturn with shear rate. Measurements at shear rates much higher than the critical shear rate were not possible because sample expulsion from the cone−plate geometry occurs. These types of flow curves look remarkably similar to the shear-induced gelation behavior observed for a variety of systems.[39,40,54−60] The time for the sample to equilibrate (i.e., yield a stable signal) was found to be on the order of a few seconds both in the Newtonian region and in the upturn. The abrupt change in behavior around the critical shear rate was found to be instantaneously reversible. After crossing over to the shear-induced gelation regime, the measurements were promptly repeated from low-to-high shear rates, commencing from the Newtonian regime. The viscosities were found to be in agreement for all consecutive measurements, indicating that the recovery is too rapid to measure.

At a fixed polymer and added salt content (c = 1 M, c_s = 2.5 M), the specific viscosity scales as $\eta_{sp} \propto M_w^3$ in the 66 kg/mol < M_w < 620 kg/mol range, suggestive of entangled dynamics. The onset of shear-thickening scales with molar mass as $\dot{\gamma}_c \sim$

https://doi.org/10.1021/acs.macromol.4c00542
Macromolecules XXXX, XXX, XXX−XXX

M^{-3}, making the critical shear stress $\sigma_c \simeq 400$ Pa independent of molar mass (see Figure S3a), which corresponds to an energy of k_BT per $\simeq 9 \times 10^3$ nm^3. Approximating the conformation of NaPSS as ideal, we use $R_g^2/N \simeq 1$ nm^2,[2] and find this volume corresponds to $1-10R_g^3$ for the M_w range plotted in Figure S3a. The critical shear stress for shear-induced gelation has previously been found to be independent of polymer concentration ($\sigma_c \sim 20$ Pa) for solutions of poly(methacrylic acid) in salt-free water.[40] For our system, however, σ_c shows a significant dependence on polyelectrolyte concentration ($\sigma_c \sim c^2$) as can be seen in Figure S3b.

The zero-shear rate viscosity displays strong dependencies on the polymer and added salt concentrations. As shown in Figures 2e,f, the zero-shear viscosity scales as

$$\eta(0) \sim M_w^3 c^{12\pm2} c_s^{13\pm1} \tag{2}$$

The polymer concentration exponent contrasts with the much weaker values observed in nonionic polymers (3.75−5) and with those observed for NaPSS in DI water in this same concentration regime ($\simeq 1.5$)[12,13] The critical shear rate displays similarly strong dependencies on the polymer and added salt concentrations

$$\dot{\gamma}_C \sim M_w^{-3} c^{-9\pm1.1} c_s^{-16\pm1} \tag{3}$$

Alternatively, the c and c_s dependence of $\eta(0)$ can also be described by exponential functions, see the Supporting Information (Figure S2). These strong dependences of the rheological parameters on solute concentration are consistent with the findings of Robin et al. for concentrated aqueous solutions of polymethacrylic acid (PMA) at 25 °C, who found that the specific viscosity and the critical shear rate scale as $\eta_{sp} \sim c^{19}$ and $\dot{\gamma}_C \sim c^{-16.5}$, respectively.[40]

Figure 3 plots the apparent viscosity of a solution ($c = 0.9$ M, $c_s = 2.5$ M) as a function of time following the application of

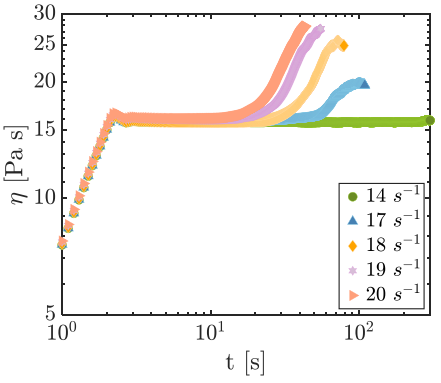

Figure 3. Evolution of viscosity (η) with time during the start-up of shear. Measurements performed at different shear rates for NaPSS with $M_w = 483$ kg/mol ($c = 0.9$ M, $c_s = 2.5$ M) in the presence of N_2 atmosphere using a stress-controlled rheometer.

different shear rates. (Note: A stress-controlled rheometer was used for these step strain-rate experiments. The strain rate vs time equilibrates to a constant value after ∼2−3s, see the Supporting Information. Similar experiments with a strain-controlled rheometer are reported on the Supporting Information.) For the lowest shear rate considered (14 s^{-1}), the viscosity stabilizes to a constant value within approximately 3s. For higher shear rates, after reaching a steady state in less than 10 s, the system becomes unstable and the apparent viscosity rapidly increases with time beyond a critical time (τ_i), which is a decreasing function of applied shear rate scaling as $\tau_i \sim \dot{\gamma}^{-5}$. Measurements were not carried out at longer times to avoid sample expulsion from the geometry. This is in qualitative agreement with the observations of Robin et al.[40] and Ono et al.[61] for polymethacrylic acid in aqueous solution, see Figure S4. The increase in the apparent viscosity indicates structure formation upon imposition of a constant strain rate.

SANS. Small angle neutron scattering measurements were carried out under zero-average contrast (ZAC) conditions. The scattering signal is therefore proportional to the form factor of the chain. When the fraction of hydrogenated and deuterated chains is set to 0.5, the ZAC scattering intensity is given by[42]

$$I(q) = N_A \overline{b_m}^2 N c P(q) \tag{4}$$

where N_A is Avogadro's constant, N is the degree of polymerization and $\overline{b_m}$ is the contrast parameter for the PSS monomer, see eqs 3 and 6 of ref 42. Note that as $N_A\overline{b_m}^2 Nc$ is known ($\simeq 1.98$ cm^{-1} for this system), the form factor $P(q)$, which describes the correlations of monomers in a single chain, can be directly calculated from the SANS measurements. The presence of NaCl affected the D_2O fraction required for the ZAC condition by less than 2%, even at a 3 M NaCl concentration.

In the low $q\xi \lesssim 1$ region, semidilute chains are not expected to be influenced by excluded volume[62] and the form factor is therefore given by the Debye function:

$$P(q) = \frac{2}{(qR_g)^4}\left[q^2R_g^2 - 1 + e^{-q^2R_g^2}\right] \tag{5}$$

where R_g is the radius of gyration of the chain.

Figure 4 plots the background subtracted scattering intensity of a NaPSS solution with a concentration of $c = 0.33$ M in

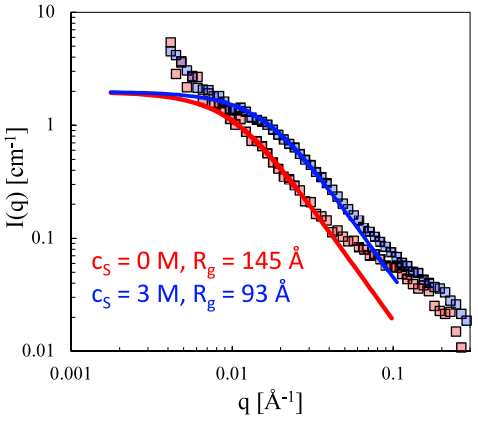

Figure 4. SANS intensity for NaPSS with $c = 0.33$ M in H_2O/D_2O mixture without added salt (red symbols) and with 3 M NaCl (blue symbols). Lines are fits to eqs 4 and 5. The only free parameter is R_g. Note that low q data are not considered in the fit.

aqueous solutions without added salt and with 3 M added NaCl. The fits to eq 5 are shown by the red and blue lines and are used to extract the radius of gyration of the chains as the sole fitting parameter. This fitting method was preferred over the Zimm or Berry methods because polyelectrolytes typically display excess scattering at low q. While this can be removed by filtration, we opted not to filter our samples due to their

https://doi.org/10.1021/acs.macromol.4c00542
Macromolecules XXXX, XXX, XXX−XXX

high sensitivity to applied shear. The decrease of the radius of gyration with increasing added salt can be seen from the fact that the scattering intensity starts decreasing at a lower q for the salt-free sample. The high-q data were not analyzed in detail here as we found that background subtraction was difficult to perform accurately, and this has a large impact on the high-q signal, where the samples scatter weakly. A further complication arises from the influence of inelastic scattering at high q, which we are not able to accurately account for. These effects do not influence the low and medium q data significantly. An evaluation of various literature studies for the crossover between $P(q) \propto q^{-2}$ and $P(q) \propto q^{-1}$ for NaPSS in aqueous solution with no added salts[11] demonstrated that chains become flexible at a length scale proportional to $c^{-1/2}$ ($\simeq$ 4 nm at c = 1 M). This is $\simeq$30% larger than the correlation length and around 4× larger than the Debye screening length, thus supporting Dobrynin et al's conjecture on electrostatic screening.[1]

DISCUSSION

Scaling Laws. Figure 5 shows the crossover between the dilute and semidilute regimes as well as the upturn salt concentration as a function of polymer concentration for two NaPSS polymers with M_w = 271 and 1010 kg/mol. The red curve represents the c_s and c combinations where the Debye screening length (κ^{-1}) is the same as the Bjerrum length (l_B). The plot also shows the Dobrynin prediction for c^* and c_s according to the following equation:[1]

$$c^*\left(1 + \frac{2c_s}{fc^*}\right)^{-1.5} \simeq N^{-2}\left(\frac{B}{b}\right)^3 \quad (6)$$

where f is the fraction of monomers with a dissociated charge, B is the stretching parameter and b is the monomer size. For NaPSS, we have used f = 0.2, B = 1.5 and b = 0.25 nm. We observe a decent agreement between the experimental data and the theoretical prediction at low and intermediate c_s. However, in the high salt limit, the measured c^* is larger than the predicted values, which means that chain dimensions decrease with added salt to a smaller degree than expected by eq 6. This probably occurs because the chains approach the neutral polymer dimensions at high c_s, so that c^* is expected to be independent or weakly dependent on c_s. Additionally, the Debye−Huckel theory, which serves as the basis for the electrostatic screening effects considered for the scaling predictions, does not hold in the $\kappa^{-1} < l_B$ limit.

The model of Dobrynin et al. predicts the end-to-end size of chains in semidilute solution to scale with added salt as

$$R(c_s) = R(0)\left[1 + \frac{2c_s}{fc}\right]^{-1/8} \quad (7)$$

where $R(0)$ is the end-to-end distance of a chain in a solution without added salt.

Figure 6 plots the radius of gyration of PSS chains normalized by the value in solution without added salt as a function of ratio of salt to polymer concentration for c = 0.33 M. Our results are found to be in close agreement with those of Spiteri,[63] who measured R_g using the zero-average contrast technique for NaPSS of similar degree of polymerization N = 780 at c = 0.34 M. The scaling prediction (eq 7) using the conductivity and osmometry[64] value of f = 0.2 is shown as a black line. The scaling model works qualitatively. The R_g values at c_s = 3 M correspond to $R_g^2/N \simeq 15.5$ Å^2[63] and $R_g^2/N \simeq 11.5$ Å^2 (our work), which are ∼20−40% higher than the dimensions of NaPSS under θ-solvent conditions.[2]

Increases in the specific viscosity with increasing added salt have been reported by Matsumoto et al. for poly(ionic liquids) in ionic-liquid/organic solvent solutions.[65−67] These data, which have been interpreted in terms of the underscreening theory of Perkin and co-workers[68,69] show qualitatively different behavior from ours in that the onset of the η_{sp} increase occurs at fixed ionic strength, so that at low polymer concentrations, $c_{s,u}$ is essentially independent of the polymer concentration, in contrast to the behavior observed in Figure 1c. No shear thickening was observed by Matsumoto et al. for any of their solutions, which always displayed shear thinning.

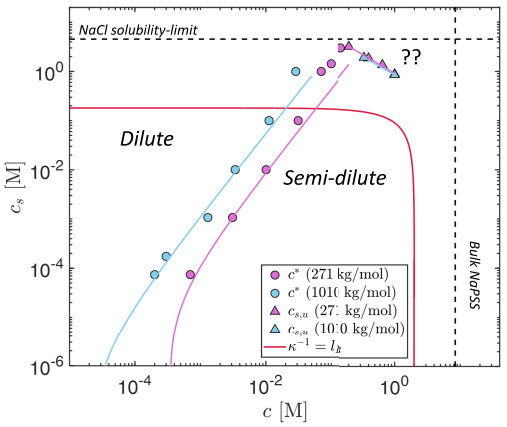

Figure 5. Overlap concentrations (c^*, circles) and upturn salt concentrations ($c_{s,u}$, triangles) for NaPSS with M_w = 271 kg/mol and 1010 kg/mol. A residual salt concentration of 7.4 × 10^{-5} M, as determined in a previous publication,[36] has been added to determine the final c_s. The horizontal dashed line represents the NaCl solubility limit in water and the vertical dashed line is the bulk NaPSS concentration. The solid blue and pink lines describe the Dobrynin predictions for the respective molar masses (eq 6), which work well until the Debye length reaches the Bjerrum length (red line). The Debye length is calculated based on the concentration of salt ions and free counterions.

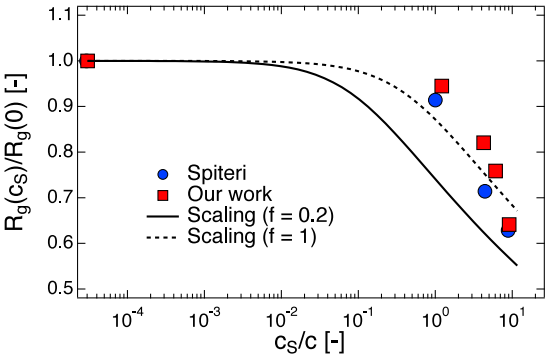

Figure 6. Chain dimensions as a function of c_S/c for NaPSS chains in water-NaCl solutions (our work, c = 0.33 M) and water-NaBr solutions (Spiteri, c = 0.34 M). Spiteri's data are from.[63] Line is the scaling prediction (eq 7) with a constant value of f = 0.2 (no free parameters), which is qualitatively correct. The scaling prediction with f = 1 is added for comparison.

https://doi.org/10.1021/acs.macromol.4c00542
Macromolecules XXXX, XXX, XXX−XXX

Our SANS experiments as well as light scattering measurements on dilute NaPSS solutions[70] do not show expansion of the chains at high c_s.

The viscosity upturns with increasing c_s are observed only for semidilute solutions, while for dilute solutions η_{sp} is a continuously decreasing function of the added salt content as shown in Figure S5. This observation is consistent with attractive forces between chain segments, which in dilute solutions lead to chain contraction and in nondilute solutions promote network formation via associative interchain interactions. The power-laws of the viscosity on polymer concentration in the $c_s > c_{s,u}$ regime, where $c_{s,u}$ is given by eq 1, are stronger than those usually observed for associative polymers.[71−75]

The $\eta_{sp} \propto M_w^3$ dependence observed for samples in the $c_s > c_{s,u}$, matches the reptation exponent for entangled linear polymers.[62] For NaPSS in DI water at c = 1 M, a previous study[13] estimated the entanglement molar mass from the crossover between the Rouse exponent ($\eta_{sp} \propto M_w$) to the reptation exponent to be $M_w \simeq 400$ kg/mol. The data plotted in Figure 2d for c_s = 2.5 M ($\simeq 2.5c_{s,u}$) by contrast show that the $\eta_{sp} \propto M_w^3$ scaling holds down to at least 66 kg/mol, which would require that the entanglement molar mass decreases by an order of magnitude by the addition of 2.5 M NaCl, in contrast to the theoretical expectation that entanglement density decreases upon chain shrinking.[1,49] Oscillatory sweeps for the 483 kg/mol polymer, plotted in Figure S8, reveal an increase of the entanglement plateau modulus (estimated from the crossover point between G' and G'') in 2.5 M NaCl relative to DI water,[13] by a factor of ≃1.3, which is insufficient to explain the apparent decrease in the entanglement molar mass or an order of magnitude. Thus, reptation dynamics do not account for the cubic dependence of the specific viscosity on the molar mass.

Shear-Induced Gelation. Robin et al.[40] have recently proposed a model treating PMA chains as soft-colloids that overlap and coalesce due to inter and intramolecular associations at high concentrations. This is in part based on the hydrophobic nature of PMA but we note that PSS could be even more hydrophobic, given the insolubility of the parent polymer (polystyrene) in water. However, the quantification of the hydrophobicity of a polymer backbone in the presence of the functional groups is not possible. Robin et al's proposed mechanism suggests an analogy with shear-induced jamming transitions observed for concentrated dispersions of hard colloids[76] (shake-gels), where shear can induce the formation of large necklace structures where colloidal particles are connected by extended polymer chains.[77] The scaling relations reported by Robin et al.[40] and Ono et al.[61] for aqueous PMA are in qualitative agreement with our findings for the aqueous NaPSS/NaCl system, indicating similarities in the rheological phenomena shown by the two systems. Robin et al. have demonstrated a strong decrease of the viscosity-concentration exponent as the charge fraction of the polymer increases.[40] This would, presumably, account for the quantitative differences observed in the scaling exponents, at least in part. Antonietti et al.[78] reported $\eta_{sp} \simeq M^{3.6}$ for soft spherical microgels in the bulk phase above the glass transition temperature. Thus, assuming a collapsed chain conformation might also explain the $\eta_{sp} \sim M^3$ dependence observed for nonentangled chains. However, as discussed above, the measurements of chain conformation using SANS show that chains remain in an expanded conformation in the high added salt region.

As salt is added to water, the Debye length decreases and it reaches the Bjerrum length of 0.71 nm at c_s = 0.18 M. Above this salt concentration, Debye−Huckel screening estimates no longer apply; average ion spacings are now only of order 1 nm. In this very high salt regime, the salt ions, sulfonate anions and countercations start to form a gel and this accounts for the sharp increase in viscosity at high salt concentrations in Figure 1a. In this picture, Figure 1c makes perfect sense, as less salt is needed to form a gel at higher polyelectrolyte concentrations. Such gels have been studied for many years, based primarily on neutralized poly(methacrylic acid).[40,79−82] The interaction of the polymer with water also appears to play some role, as the less hydrophobic neutralized poly(acrylic acid) does not form such a gel.[79] Like all associating polymers, the precise nature of the association is not yet clear but the consequences are very clear.

If samples are sheared with a salt concentration not too far below $c_{s,u}$, the polyelectrolyte coil can be stretched in the flow, effectively trading intramolecular associations for intermolecular ones, which leads to the gel formation in shear shown in Figures 2 and 3. Such a gel formation mechanism in shear flow is a very old idea: "more intermolecular bonds are likely to be formed in a field of flow",[79] and was discussed by Witten and Cohen in the context of ionomer solutions.[83] At higher shear rates, more chains are stretched and the gel transition occurs faster (Figure 3). The chains stretch at lower shear rates if (1) chain length is increased (Figure 2a), (2) polymer concentration is increased (Figure 2b) or (3) salt concentration is increased (Figure 2c). The latter presumably arises because at a given polymer concentration, adding salt brings the system closer to $c_{s,u}$ (i.e., approaching the phase boundary).

Witten and Cohen expect the existence of a positive-feedback mechanism for associating ionomers whereby shear-induced chain elongation leads to cluster formation, and cluster formation enhances the ability of shear flows to elongate chains. This is expected to lead to an instability above a threshold value of the shear rate, which is consistent with the results observed in Figures 3 and S6 for our system, and the data of Robin et al.[40] and Ono et al.[61] for PMA.

Three outstanding questions should be addressed to understand the mechanism underlying the shear-thickening of NaPSS in NaCl: at the nanoscopic level, the origin of the apparent attractive interchain interactions should be elucidated. Second, the degree to which chain alignment and/or extension occur under shear needs to be established, for example by scattering techniques under flow. Third, a direct evaluation of the chain conformation for $c_s > c_{s,u}$ in the shear thickening region should be undertaken. Measurements of single-chain conformation will necessitate rheo-SANS measurements under zero-average-contrast conditions, as carried out here under quiescent conditions.

CONCLUSIONS

The main conclusion from this study is to confirm Nobel Laureate PG de Gennes' characterization of polyelectrolytes as *'the least understood form of condensed matter'*. In contrast to the intuitive expectation that polyelectrolytes in excess salt behave like neutral polymers, we find that NaPSS in concentrated NaCl solutions displays several unusual features. At high polymer and added salt concentrations, the viscosity is found to rapidly increase with increasing added salt content, the

https://doi.org/10.1021/acs.macromol.4c00542
Macromolecules XXXX, XXX, XXX−XXX

reptation scaling of $\eta_{sp} \propto M^3$ is observed, but this scaling extends to molar masses which are too low to be entangled. Most surprisingly, solutions display strong and sudden shear thickening beyond a critical shear rate, which is reminiscent of shear-induced gelation. Neutron scattering measurements for the radius of gyration of NaPSS chains as a function of added salt qualitatively agree with the scaling theory and do not show any unexpected features. We, therefore, conclude that the strong discrepancies observed for the solution viscosity are purely dynamic in origin.

We interpret these results using the model of Witten and Cohen[83] for associative ionomer solutions, which expects that shear-induced chain elongation favors interchain contacts. The physical mechanism underlying interchain attraction for NaPSS remains unresolved, but may be the result of a crossover to an ionomer-like regime where dipolar attraction between condensed counterions becomes important. We hope this work stimulates further investigations into concentrated polyelectrolyte solutions, an area which has received relatively little attention thus far.

■ ASSOCIATED CONTENT

Supporting Information

The Supporting Information is available free of charge at https://pubs.acs.org/doi/10.1021/acs.macromol.4c00542.

Additional characterization and comparison with literature results (PDF)

Tabulated SANS, rheology, and viscosimetry data (XLSX)

■ AUTHOR INFORMATION

Corresponding Author

Carlos G. Lopez − *Institute of Physical Chemistry, RWTH Aachen University, 52056 Aachen, Germany; Department of Material Science and Engineering, The Pennsylvania State University, University Park, Pennsylvania 16802, United States;* orcid.org/0000-0001-6160-632X; Email: cvg5719@psu.edu

Authors

Anish Gulati − *Institute of Physical Chemistry, RWTH Aachen University, 52056 Aachen, Germany;* orcid.org/0000-0003-2312-5634

Aijie Han − *Department of Material Science and Engineering, The Pennsylvania State University, University Park, Pennsylvania 16802, United States;* orcid.org/0000-0002-9309-5912

Ralph H. Colby − *Department of Material Science and Engineering, The Pennsylvania State University, University Park, Pennsylvania 16802, United States;* orcid.org/0000-0002-5492-6189

Complete contact information is available at: https://pubs.acs.org/10.1021/acs.macromol.4c00542

Notes

The authors declare no competing financial interest.

■ ACKNOWLEDGMENTS

A.G. and C.G.L. thank the DFG for financial support (grant GO 3250/2-1). A.H. and R.H.C. thank the National Science Foundation for support through Chemistry-2203746. We thank the ISIS neutron source for the beamtime and Leide Cavalcanti for her help with the experiments and data reduction. We also thank Can Hou, Lars Voleske and Hannes Luhmann (RWTH) for carrying out the SANS experiments, and Arshiya Bhadu (PSU) for performing the rheo-birefringence experiments. We thank Max Hohenschutz for many useful comments.

■ REFERENCES

(1) Dobrynin, A. V.; Colby, R. H.; Rubinstein, M. Scaling theory of polyelectrolyte solutions. *Macromolecules* **1995**, *28*, 1859−1871.

(2) Lopez, C. G.; Matsumoto, A.; Shen, A. Q. Dilute polyelectrolyte solutions: recent progress and open questions. *Soft Matter* **2024**, *20*, 2635.

(3) Koene, R.; Nicolai, T.; Mandel, M. Scaling relations for aqueous polyelectrolyte-salt solutions. 3. Osmotic pressure as a function of molar mass and ionic strength in the semidilute regime. *Macromolecules* **1983**, *16*, 231−236.

(4) Noda, I.; Kato, N.; Kitano, T.; Nagasawa, M. Thermodynamic properties of moderately concentrated solutions of linear polymers. *Macromolecules* **1981**, *14*, 668−676.

(5) Colby, R. H. Structure and linear viscoelasticity of flexible polymer solutions: comparison of polyelectrolyte and neutral polymer solutions. *Rheol. Acta* **2010**, *49*, 425−442.

(6) Muthukumar, M. Phase diagram of polyelectrolyte solutions: weak polymer effect. *Macromolecules* **2002**, *35*, 9142−9145.

(7) Krause, W. E.; Tan, J. S.; Colby, R. H. Semidilute solution rheology of polyelectrolytes with no added salt. *J. Polym. Sci., Part B: Polym. Phys.* **1999**, *37*, 3429−3437.

(8) Di Cola, E.; Plucktaveesak, N.; Waigh, T.; Colby, R.; Tan, J.; Pyckhout-Hintzen, W.; Heenan, R. Structure and dynamics in aqueous solutions of amphiphilic sodium maleate-containing alternating copolymers. *Macromolecules* **2004**, *37*, 8457−8465.

(9) Di Cola, E.; Waigh, T. A.; Colby, R. H. Dynamic light scattering and rheology studies of aqueous solutions of amphiphilic sodium maleate containing copolymers. *J. Polym. Sci., Part B: Polym. Phys.* **2007**, *45*, 774−785.

(10) Lopez, C. G.; Colby, R. H.; Graham, P.; Cabral, J. T. Viscosity and scaling of semiflexible polyelectrolyte NaCMC in aqueous salt solutions. *Macromolecules* **2017**, *50*, 332−338.

(11) Lopez, C. G.; Richtering, W. Conformation and dynamics of flexible polyelectrolytes in semidilute salt-free solutions. *J. Chem. Phys.* **2018**, *148*, 244902.

(12) Lopez, C. G.; Richtering, W. Viscosity of semidilute and concentrated nonentangled flexible polyelectrolytes in salt-free solution. *J. Phys. Chem. B* **2019**, *123*, 5626−5634.

(13) Lopez, C. G. Scaling and entanglement properties of neutral and sulfonated polystyrene. *Macromolecules* **2019**, *52*, 9409−9415.

(14) Lopez, C. G. Entanglement properties of polyelectrolytes in salt-free and excess-salt solutions. *ACS Macro Lett.* **2019**, *8*, 979−983.

(15) Chen, G.; Perazzo, A.; Stone, H. A. Electrostatics, conformation, and rheology of unentangled semidilute polyelectrolyte solutions. *J. Rheol.* **2021**, *65*, 507−526.

(16) Lopez, C. G.; Linders, J.; Mayer, C.; Richtering, W. Diffusion and viscosity of unentangled polyelectrolytes. *Macromolecules* **2021**, *54*, 8088−8103.

(17) Han, A.; Uppala, V. V. S.; Parisi, D.; George, C.; Dixon, B. J.; Ayala, C. D.; Li, X.; Madsen, L. A.; Colby, R. H. Determining the Molecular Weight of Polyelectrolytes Using the Rouse Scaling Theory for Salt-Free Semidilute Unentangled Solutions. *Macromolecules* **2022**, *55*, 7148−7160.

(18) Chen, Q.; Bao, N.; Wang, J.-H. H.; Tunic, T.; Liang, S.; Colby, R. H. Linear viscoelasticity and dielectric spectroscopy of ionomer/plasticizer mixtures: A transition from ionomer to polyelectrolyte. *Macromolecules* **2015**, *48*, 8240−8252.

(19) Zhang, Z.; Liu, C.; Cao, X.; Wang, J.-H. H.; Chen, Q.; Colby, R. H. Morphological evolution of ionomer/plasticizer mixtures during a transition from ionomer to polyelectrolyte. *Macromolecules* **2017**, *50*, 963−971.

(20) Ohtani, N.; Inoue, Y.; Kaneko, Y.; Okumura, S. Solution viscosity behavior of polystyrene-based cationic ionomers: Effects of quaternary-group structure and counter ion. *J. Polym. Sci., Part A: Polym. Chem.* **1995**, *33*, 2449−2454.
(21) Ohtani, N.; Inoue, Y.; Kaneko, Y.; Sakakida, A.; Takeishi, I.; Furutani, H. Solution viscosity behavior and swelling behavior of polystyrene-based cationic ionomers. Effects of added salts and counterion. *Polym. J.* **1996**, *28*, 11−15.
(22) Chen, Q.; Tudryn, G. J.; Colby, R. H. Ionomer dynamics and the sticky Rouse model. *J. Rheol.* **2013**, *57*, 1441−1462.
(23) Nomula, S.; Cooper, S. L. Ionomer solution structure and solution diagram. *Macromolecules* **2001**, *34*, 2653−2659.
(24) Pfeuty, P. Conformation des polyelectrolytes ordre dans les solutions de polyelectrolytes. *J. Phys. Colloques* **1978**, *39*, C2-149.
(25) Chen, G.; Perazzo, A.; Stone, H. A. Influence of salt on the viscosity of polyelectrolyte solutions. *Phys. Rev. Lett.* **2020**, *124*, 177801.
(26) Lopez, C. G.; Horkay, F.; Mussel, M.; Jones, R. L.; Richtering, W. Screening lengths and osmotic compressibility of flexible polyelectrolytes in excess salt solutions. *Soft Matter* **2020**, *16*, 7289−7298.
(27) Iwamoto, Y.; Hirose, E.; Norisuye, T. Electrostatic contributions to chain stiffness and excluded-volume effects in sodium poly (styrenesulfonate) solutions. *Polym. J.* **2000**, *32*, 428−434.
(28) Hayashi, K.; Tsutsumi, K.; Norisuye, T.; Teramoto, A. Electrostatic contributions to chain stiffness and excluded-volume effects in sodium hyaluronate solutions. *Polym. J.* **1996**, *28*, 922−928.
(29) Yashiro, J.; Hagino, R.; Sato, S.; Norisuye, T. Chain stiffness and excluded-volume effects in polyelectrolyte solutions: characterization of sodium poly (2-acrylamido-2-methylpropanesulfonate) in aqueous sodium chloride. *Polym. J.* **2006**, *38*, 57−63.
(30) Yashiro, J.; Norisuye, T. Excluded-volume effects on the chain dimensions and transport coefficients of sodium poly (styrene sulfonate) in aqueous sodium chloride. *J. Polym. Sci., Part B: Polym. Phys.* **2002**, *40*, 2728−2735.
(31) Hagino, R.; Yashiro, J.; Sakata, M.; Norisuye, T. Electrostatic contributions to chain stiffness and excluded-volume effects in sodium poly (2-acrylamido-2-methylpropanesulfonate) solutions. *Polym. J.* **2006**, *38*, 861−867.
(32) Tsutsumi, K.; Norisuye, T. Excluded-volume effects in sodium hyaluronate solutions revisited. *Polym. J.* **1998**, *30*, 345−349.
(33) Sharratt, W. N.; O'Connell, R.; Rogers, S. E.; Lopez, C. G.; Cabral, J. T. Conformation and phase behavior of sodium carboxymethyl cellulose in the presence of mono-and divalent salts. *Macromolecules* **2020**, *53*, 1451−1463.
(34) Boris, D. C.; Colby, R. H. Rheology of sulfonated polystyrene solutions. *Macromolecules* **1998**, *31*, 5746−5755.
(35) Lopez, C. G. Entanglement of semiflexible polyelectrolytes: Crossover concentrations and entanglement density of sodium carboxymethyl cellulose. *J. Rheol.* **2020**, *64*, 191−204.
(36) Gulati, A.; Jacobs, M.; Lopez, C. G.; Dobrynin, A. V. Salt Effect on the Viscosity of Semidilute Polyelectrolyte Solutions: Sodium Polystyrenesulfonate. *Macromolecules* **2023**, *56*, 2183−2193.
(37) Bossis, G.; Brady, J. The rheology of Brownian suspensions. *J. Chem. Phys.* **1989**, *91*, 1866−1874.
(38) Lee, Y. S.; Wagner, N. J. Dynamic properties of shear thickening colloidal suspensions. *Rheol. Acta* **2003**, *42*, 199−208.
(39) Wang, J.; Benyahia, L.; Chassenieux, C.; Tassin, J.-F.; Nicolai, T. Shear-induced gelation of associative polyelectrolytes. *Polymer* **2010**, *51*, 1964.
(40) Robin, C.; Lorthioir, C.; Amiel, C.; Fall, A.; Ovarlez, G.; Le Cœur, C. Unexpected rheological behavior of concentrated poly (methacrylic acid) aqueous solutions. *Macromolecules* **2017**, *50*, 700−710.
(41) Lopez, C. G.; Horkay, F.; Schweins, R.; Richtering, W. Solution properties of polyelectrolytes with divalent counterions. *Macromolecules* **2021**, *54*, 10583−10593.
(42) Kassapidou, K.; Jesse, W.; Kuil, M.; Lapp, A.; Egelhaaf, S.; Van der Maarel, J. Structure and charge distribution in DNA and poly (styrenesulfonate) aqueous solutions. *Macromolecules* **1997**, *30*, 2671−2684.
(43) Ise, N.; Okubo, T. Partial Molal Volume of Polyelectrolytes. *J. Am. Chem. Soc.* **1968**, *90*, 4527−4533.
(44) Parisi, D.; Han, A.; Seo, J.; Colby, R. H. Rheological response of entangled isotactic polypropylene melts in strong shear flows: Edge fracture, flow curves, and normal stresses. *J. Rheol.* **2021**, *65*, 605−616.
(45) Reddy, M.; Marinsky, J. A. Further investigation of the osmotic properties of hydrogen and sodium polystyrenesulfonates. *J. Phys. Chem.* **1970**, *74*, 3884−3891.
(46) Eisenberg, H.; Mohan, G. R. Aqueous Solutions of Polyvinylsulfonic Acid: Phase Separation and Specific. Interactions with Ions, Viscosity, Conductance and Potentiometry. *J. Phys. Chem.* **1959**, *63*, 671−680.
(47) Eisenberg, H.; Casassa, E. F. Aqueous solutions of salts of poly (vinylsulfonic acid). *J. Polym. Sci.* **1960**, *47*, 29−44.
(48) Eisenberg, H.; Woodside, D. Multicomponent polyelectrolyte solutions. Part II. Excluded volume study of polyvinylsulfonate alkali halide systems. *J. Chem. Phys.* **1962**, *36*, 1844−1854.
(49) Dobrynin, A. V.; Jacobs, M. When do polyelectrolytes entangle? *Macromolecules* **2021**, *54*, 1859−1869.
(50) Han, A.; Colby, R. H. Rheology of entangled polyelectrolyte solutions. *Macromolecules* **2021**, *54*, 1375−1387.
(51) Lopez, C. G.; Rogers, S. E.; Colby, R. H.; Graham, P.; Cabral, J. T. Structure of sodium carboxymethyl cellulose aqueous solutions: A SANS and rheology study. *J. Polym. Sci., Part B: Polym. Phys.* **2015**, *53*, 492−501.
(52) Colby, R.; Boris, D.; Krause, W.; Dou, S. Shear thinning of unentangled flexible polymer liquids. *Rheol. Acta* **2007**, *46*, 569−575.
(53) Stratton, R. A. Non-Newtonian flow in polymer systems with no entanglement coupling. *Macromolecules* **1972**, *5*, 304−310.
(54) Liu, C. H.; Pine, D. Shear-Induced Gelation and Fracture in Micellar Solutions. *Phys. Rev. Lett.* **1996**, *77*, 2121−2124.
(55) Gagnon, D. A.; Dessi, C.; Berezney, J. P.; Boros, R.; Chen, D. T.-N.; Dogic, Z.; Blair, D. L. Shear-Induced Gelation of Self-Yielding Active Networks. *Phys. Rev. Lett.* **2020**, *125*, 178003.
(56) Kjøniksen, A.-L.; Hiorth, M.; Roots, J.; Nystrom, B. Shear-Induced Association and Gelation of Aqueous Solutions of Pectin. *J. Phys. Chem. B* **2003**, *107*, 6324−6328.
(57) Bercea, M.; Gradinaru, L.-M.; Barbalata-Mandru, M.; Vlad, S.; Nita, L. E.; Plugariu, I.-A.; Albulescu, R. Shear flow of associative polymers in aqueous solutions. *J. Mol. Struct.* **2021**, *1238*, 130441.
(58) Cadix, A.; Chassenieux, C.; Lafuma, F.; Lequeux, F. Control of the Reversible Shear-Induced Gelation of Amphiphilic Polymers through Their Chemical Structure. *Macromolecules* **2005**, *38*, 527−536.
(59) Lele, A.; Shedge, A.; Badiger, M.; Wadgaonkar, P.; Chassenieux, C. Abrupt Shear Thickening of Aqueous Solutions of Hydrophobically Modified Poly(N,N'-dimethylacrylamide-co-acrylic acid). *Macromolecules* **2010**, *43*, 10055−10063.
(60) Khandavalli, S.; Park, J. H.; Winter, H. H.; Myers, D. J.; Ulsh, M.; Mauger, S. A. Viscoelasticity Enhancement and Shear Thickening of Perfluorinated Sulfonic Acid Ionomer Dispersions in Water−Alcohol Solvent Mixtures. *Macromolecules* **2023**, *56*, 6988−7005.
(61) Ono, K.; Murakami, K. Kinetics of gelation of aqueous poly (methacrylic acid) solutions under shear stress. *J. Polym. Sci., Polym. Lett. Ed.* **1977**, *15*, 507−511.
(62) Colby, R. H.; Rubinstein, M. *Polymer Physics*; Oxford University Press: New York, 2003.
(63) Spiteri, M. Conformation et correlations spatiales dans les solutions de polyelectrolytes: etude par Diffusion de Neutrons aux Petits Angles. Ph.D. Thesis, Université de Paris-Sud Orsay, 1997.
(64) Bordi, F.; Cametti, C.; Colby, R. Dielectric spectroscopy and conductivity of polyelectrolyte solutions. *J. Phys.: Condens. Matter* **2004**, *16*, R1423.
(65) Matsumoto, A.; Del Giudice, F.; Rotrattanadumrong, R.; Shen, A. Q. Rheological scaling of ionic-liquid-based polyelectrolytes in ionic liquid solutions. *Macromolecules* **2019**, *52*, 2759−2771.

https://doi.org/10.1021/acs.macromol.4c00542
Macromolecules XXXX, XXX, XXX−XXX

(66) Matsumoto, A.; Yoshizawa, R.; Urakawa, O.; Inoue, T.; Shen, A. Q. Rheological Scaling of Ionic Liquid-Based Polyelectrolytes in the Semidilute Unentangled Regime from Low to High Salt Concentrations. *Macromolecules* **2021**, *54*, 5648−5661.
(67) Matsumoto, A.; Shen, A. Q. Rheological scaling of ionic-liquid-based polyelectrolytes in ionic liquid solutions: the effect of the ion diameter of ionic liquids. *Soft Matter* **2022**, *18*, 4197−4204.
(68) Lee, A. A.; Perez-Martinez, C. S.; Smith, A. M.; Perkin, S. Underscreening in concentrated electrolytes. *Faraday Discuss.* **2017**, *199*, 239−259.
(69) Smith, A. M.; Lee, A. A.; Perkin, S. The electrostatic screening length in concentrated electrolytes increases with concentration. *J. Phys. Chem. Lett.* **2016**, *7*, 2157−2163.
(70) Hirose, E.; Iwamoto, Y.; Norisuye, T. Chain stiffness and excluded-volume effects in sodium poly (styrenesulfonate) solutions at high ionic strength. *Macromolecules* **1999**, *32*, 8629−8634.
(71) Lopez, C. G.; Colby, R. H.; Cabral, J. T. Electrostatic and hydrophobic interactions in NaCMC aqueous solutions: Effect of degree of substitution. *Macromolecules* **2018**, *51*, 3165−3175.
(72) Barba, C.; Montané, D.; Farriol, X.; Desbrières, J.; Rinaudo, M. Synthesis and characterization of carboxymethylcelluloses from non-wood pulps II. Rheological behavior of CMC in aqueous solution. *Cellulose* **2002**, *9*, 327−335.
(73) Kujawa, P.; Audibert-Hayet, A.; Selb, J.; Candau, F. Rheological properties of multisticker associative polyelectrolytes in semidilute aqueous solutions. *J. Polym. Sci., Part B: Polym. Phys.* **2004**, *42*, 1640−1655.
(74) Kujawa, P.; Audibert-Hayet, A.; Selb, J.; Candau, F. Effect of ionic strength on the rheological properties of multisticker associative polyelectrolytes. *Macromolecules* **2006**, *39*, 384−392.
(75) Aoki, K.; Sugawara-Narutaki, A.; Doi, Y.; Takahashi, R. Structure and rheology of poly (vinylidene difluoride-co-hexafluoropropylene) in an ionic liquid: The solvent behaves as a weak cross-linker through ion−dipole interaction. *Macromolecules* **2022**, *55*, 5591−5600.
(76) Holmes, C. B.; Cates, M. E.; Fuchs, M.; Sollich, P. Glass transitions and shear thickening suspension rheology. *J. Rheol.* **2005**, *49*, 237−269.
(77) Cabane, B.; Wong, K.; Lindner, P.; Lafuma, F. Shear induced gelation of colloidal dispersions. *J. Rheol.* **1997**, *41*, 531−547.
(78) Antonietti, M.; Pakula, T.; Bremser, W. Rheology of small spherical polystyrene microgels: a direct proof for a new transport mechanism in bulk polymers besides reptation. *Macromolecules* **1995**, *28*, 4227−4233.
(79) Eliassaf, J.; Silberberg, A.; Katchalsky, A. Negative thixotropy of aqueous solutions of polymethacrylic acid. *Nature* **1955**, *176*, 1119−1119.
(80) Eliassaf, J.; Silberberg, A. The gelation of aqueous solutions of polymethacrylic acid. *Polymer* **1962**, *3*, 555−564.
(81) Ohya, S.; Matsuo, T. Time-dependent change of viscosity in polymethacrylic acid solution. *J. Colloid Interface Sci.* **1979**, *68*, 593−595.
(82) Myasnikov, B.; Trapeznikov, A.; Ryabov, A.; Yemel'yanov, D. The rheological features of concentrated polyelectrolyte solutions. *Polymer Science USSR* **1971**, *13*, 1006−1013.
(83) Witten, T., Jr; Cohen, M. H. Crosslinking in shear-thickening ionomers. *Macromolecules* **1985**, *18*, 1915−1918.

https://doi.org/10.1021/acs.macromol.4c00542
Macromolecules XXXX, XXX, XXX−XXX